Efficient 5-OP-RU-Induced Enrichment of Mucosa-Associated Invariant T Cells in the Murine Lung Does Not Enhance Control of Aerosol *Mycobacterium tuberculosis* Infection

Charles Kyriakos Vorkas,[a,b] Olivier Levy,[b] Miroslav Skular,[b] Kelin Li,[c] Jeffrey Aubé,[c] Michael S. Glickman[b,d]

[a]Division of Infectious Diseases, Weill Cornell Medicine, Cornell University, New York, New York, USA
[b]Immunology Program, Sloan Kettering Institute, Memorial Sloan Kettering Cancer Center, New York, New York, USA
[c]Division of Chemical Biology and Medicinal Chemistry, UNC Eshelman School of Pharmacy, University of North Carolina at Chapel Hill, Chapel Hill, North Carolina, USA
[d]Division of Infectious Diseases, Memorial Sloan Kettering Cancer Center, New York, New York, USA

ABSTRACT Mucosa-associated invariant T (MAIT) cells are an innate-like T cell subset in mammals that recognize microbial vitamin B metabolites presented by the evolutionarily conserved major histocompatibility complex class I (MHC I)-related molecule, MR1. Emerging data suggest that MAIT cells may be an attractive target for vaccine-induced protection against bacterial infections because of their rapid cytotoxic responses at mucosal services to a widely conserved bacterial ligand. In this study, we tested whether a MAIT cell priming strategy could protect against aerosol *Mycobacterium tuberculosis* infection in mice. Intranasal costimulation with the lipopeptide Toll-like receptor (TLR)2/6 agonist, Pam2Cys (P2C), and the synthetic MR1 ligand, 5-OP-RU, resulted in robust expansion of MAIT cells in the lung. Although MAIT cell priming significantly enhanced MAIT cell activation and expansion early after *M. tuberculosis* challenge, these MAIT cells did not restrict *M. tuberculosis* bacterial load. MAIT cells were depleted by the onset of the adaptive immune response, with decreased detection of granzyme B^+ and gamma interferon (IFN-γ)$^+$ MAIT cells relative to that in uninfected P2C/5-OP-RU-treated mice. Decreasing the infectious inoculum, varying the time between priming and aerosol infection, and testing MAIT cell priming in nitric oxide synthase 2 (NOS2)-deficient mice all failed to reveal an effect of P2C/5-OP-RU-induced MAIT cells on *M. tuberculosis* control. We conclude that intranasal MAIT cell priming in mice induces early MAIT cell activation and expansion after *M. tuberculosis* exposure, without attenuating *M. tuberculosis* growth, suggesting that MAIT cell enrichment in the lung is not sufficient to control *M. tuberculosis* infection.

KEYWORDS innate immunity, MAIT cells, tuberculosis

Mucosa-associated invariant T (MAIT) cells are an evolutionarily conserved innate-like T cell subset in mammals that recognize microbially derived vitamin B intermediates presented by the monomorphic major histocompatibility complex class I (MHC I)-related molecule, MR1 (1, 2). Unlike conventional T cells, MAIT cells are activated within hours of antigen recognition (3, 4) and "licensed" to kill bacterially infected cells (5, 6). MAIT cells also secrete cytokines that recruit accessory immune cells during bacterial infection (7–9). These characteristics suggest that enhancing MAIT cell numbers or function may be an attractive pan-bacterial vaccine approach (10).

MAIT cell responses have been documented in a number of infectious and noninfectious inflammatory diseases (2, 11), including the leading infectious cause of death globally, tuberculosis (TB) (3, 12–19). Peripheral blood MAIT cells contract during active TB disease (13, 17, 18, 20) and are activated during acute exposure in healthy house-

Citation Vorkas CK, Levy O, Skular M, Li K, Aubé J, Glickman MS. 2021. Efficient 5-OP-RU-induced enrichment of mucosa-associated invariant T cells in the murine lung does not enhance control of aerosol *Mycobacterium tuberculosis* infection. Infect Immun 89:e00524-20. https://doi.org/10.1128/IAI.00524-20.

Editor Liise-anne Pirofski, Albert Einstein College of Medicine

Address correspondence to Michael S. Glickman, glickmam@mskcc.org.

Received 18 August 2020
Returned for modification 21 September 2020
Accepted 6 October 2020
Accepted manuscript posted online 15 October 2020
Published 15 December 2020

hold contacts (3, 15). Limited studies of lung pathology in TB patients suggest that MAIT cells may be recruited to the lungs during active infection (21, 22). Better understanding of the role of MAIT cells in host defenses against *Mycobacterium tuberculosis in vivo* will be critical to assessing their contribution to protective immunity, yet few studies have examined the role of MAIT cell responses using *in vivo* animal models of tuberculosis (23–25). This previous work is consistent with limited MAIT cell activation and proliferation after *M. tuberculosis* infection relative to the significant expansion of *M. tuberculosis* antigen-specific T cells.

In vivo modeling of MAIT cell responses against *M. tuberculosis* has been limited by low MAIT cell abundance in specific-pathogen-free (SPF) mice (<1% of T cells) relative to the generally more abundant MAIT cell populations observed in humans (<1% to 18% of T cells) (2, 26, 27). Despite low abundance of MAIT cell populations in SPF mice, several recent studies demonstrate that intranasal priming with bacteria or synthetic MR1 ligands can induce rapid and robust MAIT cell proliferation in the lungs (27–31). Murine pulmonary MAIT cells significantly expand after intranasal inoculation of *Salmonella enterica* serovar Typhimurium, *Francisella tularensis*, or *Legionella longbeachae* in an MR1-dependent manner (29, 30, 32, 33). Importantly, murine pulmonary MAIT cells also expand after intranasal priming with synthetic MR1 ligand 5-OP-RU plus Toll-like receptor (TLR) ligand costimulation but not with 5-OP-RU or TLR ligands alone (29). This costimulatory priming strategy is protective against murine pulmonary *L. longbeachae* infection (30). Taken together, these data support the hypothesis that MR1 ligand-induced MAIT cell populations may protect against other intracellular pulmonary pathogens, including *Mycobacterium tuberculosis* (34, 35). Here, we assessed a MAIT cell priming strategy in the murine model of aerosol *M. tuberculosis* infection.

In the following experiments, we tested the hypothesis that MAIT cell priming with a synthetic lipopeptide TLR2/6 agonist, Pam2Cys (P2C), plus 5-OP-RU costimulation can attenuate aerosol *M. tuberculosis* infection in mice. We demonstrate that vaccination with P2C/5-OP-RU prior to *M. tuberculosis* challenge enhanced MAIT cell activation and expansion by 7 days after infection. Despite significant recruitment to the lungs after acute bacterial exposure, MAIT cells were depleted by week 3 postinfection, and no attenuation of bacterial load was observed. Decreasing the infectious inoculum, the time between priming and *M. tuberculosis* aerosol challenge, and ablating host nitric oxide synthase 2 (NOS2) all failed to reveal a salutary effect of MAIT cell priming. Our study demonstrates that MAIT cell priming enhances MAIT cell number and activation in the *M. tuberculosis*-infected lung but does not attenuate the course of infection.

RESULTS

MAIT cells respond to acute *M. tuberculosis* challenge with limited expansion in the lung and mediastinal lymph node during the chronic phase of infection. We first infected wild-type C57BL/6 (WT) mice from Jackson Laboratories with "low-dose" (LD) *M. tuberculosis* inoculum (50 to 150 CFU/lung) via the aerosol route and quantified MAIT cell abundance and activation by flow cytometry 7 and 21 days following infection. The MAIT cell gating strategy is defined in Fig. S1a in the supplemental material, and all MR1-5-OP-RU tetramer staining was controlled with MR1-6FP tetramers. As previously reported, MAIT cells are rare in SPF mice (<1%) but can be identified using MR1-5-OP-RU tetramers (26) and were most clearly detected in inguinal lymph nodes in uninfected mice (Fig. 1a and b). Seven days following *M. tuberculosis* infection, there was no significant expansion of MAIT cell subsets, and in fact, we observed fewer MAIT cells in the spleens and inguinal lymph nodes (Fig. 1b) in infected mice with a trend toward depletion in the lungs in the most prevalent double-negative (DN) subset (Fig. 1c). This was accompanied by relative enrichment in the minor $CD4^+$ subset (Fig. 1c). There was also a trend toward increased MAIT cell activation marker expression in infected mice, though this did not reach statistical significance (Fig. 1d). By 21 days postinfection, MAIT cells expanded in infected lungs and mediastinal lymph nodes (Fig. 1e and f). In the lungs, the DN MAIT cell subset underwent the most significant expansion, but increased MAIT cell numbers were also noted in $CD4^+$ and $CD8^+$ MAIT

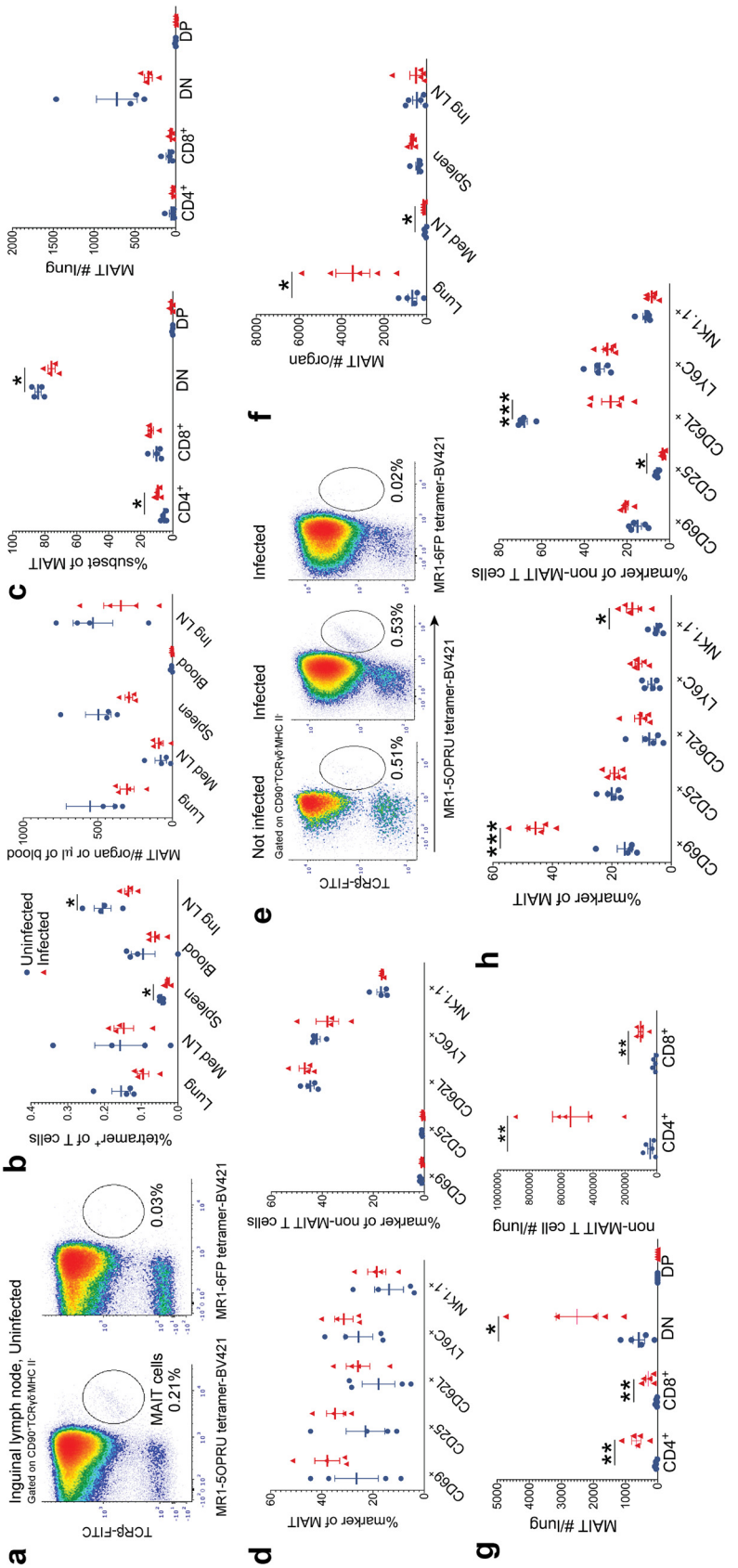

FIG 1 MAIT cells respond to *Mycobacterium tuberculosis* infection in mice. (a) Representative flow cytometry density plots from one mouse, identifying MAIT cells using MR1-5-OP-RU tetramers in the

(Continued on next page)

cell subsets (Fig. 1g). As expected, non-MAIT cells significantly expanded in lung at the onset of the adaptive immune response, most notable in the $CD4^+$ T cell subset (Fig. 1g). Pulmonary MAIT cells from mice infected for 21 days upregulated activation marker CD69 and natural killer receptor NK1.1 relative to that in uninfected mice (Fig. 1h). As expected during the adaptive response to *M. tuberculosis* infection, pulmonary non-MAIT cells strongly downregulated the naive L-selectin marker, CD62L. These data are consistent with previous findings (23–25) demonstrating that MAIT cells respond to acute *M. tuberculosis* challenge but undergo limited expansion at the onset of the adaptive immune response.

Intranasal priming with 5-OP-RU and TLR2/6 ligand Pam2Cys costimulation induces robust MAIT cell expansion within the lung. To ask whether enhancement of MAIT cell numbers or function could affect *M. tuberculosis* infection, we adapted a model of MAIT cell priming (29, 30), which is summarized in Fig. 2a. For all priming experiments, we used WT C57BL/6 mice from Taconic Laboratories due to higher lung MAIT cell numbers detected at baseline than in mice from other vendors (see Fig. S2a and b in the supplemental material). The gating strategy for all subsequent experiments is defined in Fig. S1b.

In vitro, 5-OP-RU alone was sufficient to expand splenic MAIT cells (see Fig. S3a and b). However, *in vivo*, TLR costimulation with 5-OP-RU was necessary for efficient MAIT cell expansion in the lung (29) (Fig. 2b to d; Fig. S3c). First, we confirmed that intranasal administration of MR1 ligand 5-OP-RU plus TLR2/6 ligand Pam2Cys (P2C) induces a dose-dependent MAIT cell expansion in the lung (Fig. 2b and c) and, to a lesser extent, the spleen (Fig. 2d). In contrast, P2C/5-OP-RU priming via oral gavage did not induce MAIT cell expansion (Fig. S3c). Transient MAIT cell expansion after intranasal priming was also observed in mediastinal and inguinal lymph nodes as well as blood (Fig. 2e), but relatively few MAIT cells were detected in other organs (Fig. S3d). Functionally, pulmonary and splenic MAIT cells upregulated IL-17 more than gamma interferon (IFN-γ) after *ex vivo* restimulation with 5-OP-RU (Fig. 2f to h). These experiments demonstrate efficient induction of pulmonary MAIT cell proliferation and effector function by exogenous ligand administration and replicate published studies (29, 30).

5-OP-RU plus Pam2Cys priming induces early MAIT cell activation and expansion in *M. tuberculosis*-infected lung without attenuating bacterial load. We next tested this MAIT cell priming model as a preventive strategy against *M. tuberculosis* infection. Mice were primed via intranasal inoculation and infected with 50 to 150 CFU/lung via aerosol 14 days after initiation of priming, as summarized in Fig. 3a. Increased numbers of MAIT cells in the lungs, both as a percentage of total T cells and absolute numbers, were detected in P2C/5-OP-RU-primed mice at day 7 postinfection compared to those from either infected P2C controls or uninfected P2C/5-OP-RU mice (Fig. 3b), consistent with enhanced MAIT cell activation and expansion during acute infection with vaccination. The inverse trend was observed later in infection, where P2C/5-OP-RU-treated infected mice had fewer MAIT cells in the lungs than P2C/5-OP-RU-treated but uninfected mice, consistent with depletion of MAIT cells during later

FIG 1 Legend (Continued)
inguinal lymph node compared to negative-control MR1-6FP tetramers. (b) Mean percentages of tetramer-positive MAIT cells of $CD90^+$ cells ± standard errors of the means (SEMs) and the mean MAIT cell absolute numbers ± SEMs within tissues of uninfected and *Mycobacterium tuberculosis*-infected mice 7 days postinfection. blue, not infected; red, infected; LN, lymph node. (c) MAIT cell $CD4^+$ or $CD8^+$ coexpression as mean percentages of total MAIT cells ± SEMs and mean absolute numbers ± SEMs 7 days postinfection. DN, double negative; DP, double positive. (d) Mean percent activation $marker^+$ ± SEMs of pulmonary MAIT cells and non-MAIT cells 7 days postinfection. (e) Representative flow cytometry density plots from one infected mouse 21 days after aerosol challenge and one uninfected mouse, identifying pulmonary MAIT cells using MR1-5-OP-RU tetramers. Staining was controlled using MR1-6FP tetramers. (f) Mean MAIT cell absolute numbers ± SEMs in various tissues 21 days postinfection. n = 5 mice/group. (g) Mean absolute numbers ± SEMs of MAIT cell and non-MAIT cell subsets 21 days postinfection. (h) Mean percent activation $marker^+$ ± SEMs of MAIT and non-MAIT cells 21 days postinfection. n = 4 to 5 mice/group. All data in this figure represent one independent experiment. Statistical analyses were performed using unpaired t tests. *, $P < 0.05$; **, $P < 0.005$; ***, $P < 0.0005$.

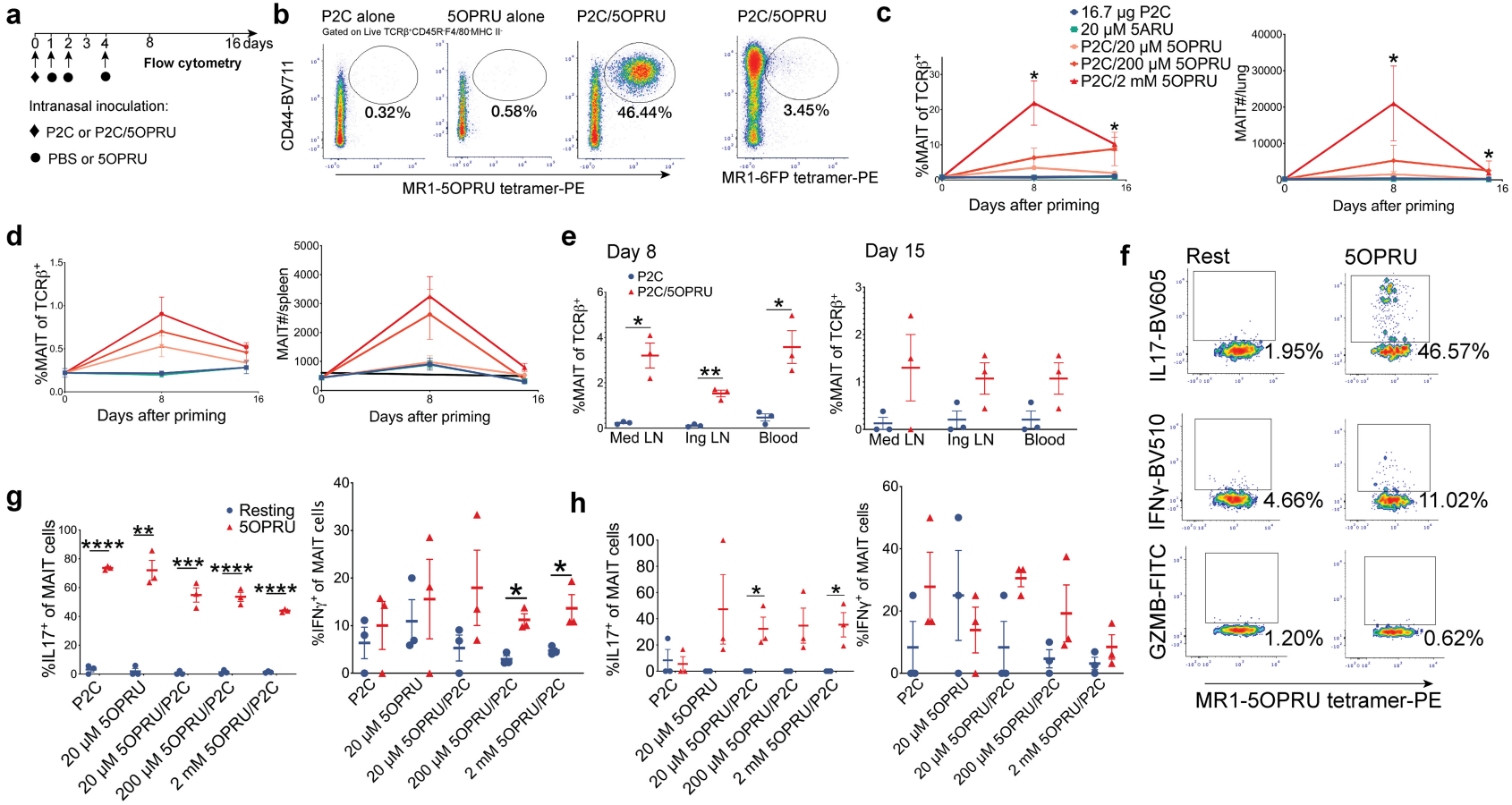

FIG 2 Pulmonary MAIT cells expand after intranasal inoculation with MR1 ligand (5-OP-RU) and Toll-like receptor 2/6 ligand (Pam2Cys) costimulation. (a) Experimental schematic of intranasal priming model for

(Continued on next page)

phases of infection. By day 7 postinfection, P2C/5-OP-RU-treated mice had blunted MAIT cell IFN-γ and granzyme B responses to 5-OP-RU restimulation *in vitro* compared to that in uninfected mice (Fig. 3c).

We next asked whether MAIT cell priming could enhance antigen-specific T cell responses by quantitating ESAT-6 and TB10.4 *M. tuberculosis*-specific T cells using MHC tetramers. The gating strategy for antigen-specific T cells is defined in Fig. S3. No difference in abundance of ESAT-6 or TB10.4 antigen-specific T cells was detected in the lungs or spleens of P2C/5-OP-RU-primed mice by days 22 or 29 postinfection (Fig. 3d and e) compared to that in infected mice treated with P2C alone. Consistent with previous observations (24), antigen-specific T cells greatly outnumbered MAIT cells in the lung during chronic infection. Although we observed a small difference in *M. tuberculosis* bacterial load immediately after aerosol deposition in P2C/5-OP-RU-treated mice, this difference was not sustained, such that bacterial loads during chronic infection in the lungs or spleens were the same in both groups (Fig. 3f and g).

Decreasing the *M. tuberculosis* inoculum or shortening the time to infection after priming did not enhance MAIT cell-mediated control of *M. tuberculosis*. We hypothesized that the low-dose *M. tuberculosis* inoculum targeting 50 to 150 CFU/lung was still higher than the physiologic inoculum of natural human infection (36, 37) and could overwhelm early effector functions of MAIT cells. We therefore compared our standard low-dose (LD) inoculum targeting 50 to 150 CFU/lung with an "ultralow-dose" (ULD) inoculum targeting 1 to 10 CFU/mouse (Fig. 4a). Using the ULD inoculum, some mice receiving aerosol challenge may remain uninfected. Although we observed fewer CFU in the lung 21 days postinfection when using the ULD than when using the LD inoculum, P2C/5-OP-RU priming did not decrease bacterial load with either inoculum (Fig. 4b).

Due to the transient kinetics of MAIT cell expansion after priming, we also hypothesized that the timing of infection after P2C/5-OP-RU treatment may impact the efficacy of our vaccination strategy. We subsequently compared two infection schedules using the ULD inoculum, conducting aerosol challenge 7 (D-7) or 14 (D-14) days after the initiation of priming (Fig. 4c). Significantly increased MAIT cell numbers in the lung were observed using the D-7 infection schedule (Fig. 4d) compared to that with the D-14 schedule. This enhanced MAIT cell enrichment was accompanied by a significant increase in TB10.4-specific $CD8^+$ T cells and decreased PD-1 expression on $CD4^+$ T cells (Fig. 4e and f) relative to that with the D-14 infection schedule. However, despite this enhanced MAIT cell and antigen-specific T cell accumulation, P2C/5-OP-RU priming again had no impact on bacterial load (Fig. 4g and h). As a subset of mice remained uninfected after ULD *M. tuberculosis* aerosol challenge, we compared the fractions of infected mice in each group, reasoning that MAIT cell priming might abort infection completely in some mice. However, we detected no significant differences across treatment groups and time points (Fig. 4i and j).

We also note that P2C/5-OP-RU priming had no significant effect on the expansion of other immune subsets during infection, including non-MAIT $CD4^+$ or $CD8^+$, γδ T, B,

FIG 2 Legend (Continued)
pulmonary MAIT cell expansion. (b) Representative flow cytometry density plots from lungs of three mice 8 days after intranasal priming under different conditions. Pulmonary MAIT cells were identified using MR1-5-OP-RU tetramers. Staining was controlled using MR1-6FP tetramers. Mean percent MAIT cells of T cells ± SEMs and mean MAIT cell absolute numbers ± SEMs measured at baseline and then 8 and 15 days after priming under different conditions in the lung (c) and spleen (d). Statistically significant results shown compare P2C/2 mM 5-OP-RU with P2C alone. (e) Mean percent MAIT of T cells ± SEMs in lymph nodes and blood at day 8 or 15 following priming with 2 μM 5-OP-RU/16.7 μg (Pam2Cys) P2C or P2C alone. (f) Representative flow cytometry density plots demonstrating intracellular cytokine staining of pulmonary MAIT cells for IL-17, IFN-γ, or granzyme B. MAIT cells were isolated 15 days after intranasal priming with 16.7 μg P2C/2 mM 5-OP-RU and then incubated *in vitro* for 15 h at rest or in the presence of 2 μM 5-OP-RU. Intracellular staining of IL-17 and IFN-γ in pulmonary (g) and splenic (h) MAIT cells incubated under the same *in vitro* conditions as described for panel f. $n = 3$ mice/group. Each panel is representative of three independent experiments. Statistical analyses were performed using unpaired *t* tests. *, $P < 0.05$; **, $P < 0.005$; ***, $P < 0.0005$; ****, $P < 0.0001$; GZMB, granzyme B; 5ARU, 5-amino-6-D-ribitylaminouracil.

FIG 3 Intranasal priming with P2C/5-OP-RU prior to *M. tuberculosis* infection induces early MAIT cell expansion and effector function without impacting bacterial load. (a) Experimental schematic of MAIT

(Continued on next page)

NK, or myeloid cells (data not shown). *M. tuberculosis* CFU did not significantly correlate with the absolute number of MAIT cells or any other immune subset in P2C/5-OP-RU-treated mice (data not shown).

In the absence of infection, we observed that MAIT cells strongly upregulated the checkpoint inhibitor PD-1 with serial P2C/5-OP-RU treatments without any additive effects on proliferation (see Fig. S5a to c). Together, these results demonstrate that priming with the synthetic ligand may drive MAIT cells to phenotypic and functional exhaustion.

MAIT cell priming does not rescue hypersusceptible NOS2-deficient mice from lethal infection. We next hypothesized that MAIT cell priming could attenuate *M. tuberculosis* infection in genetically hypersusceptible mice deficient in inducible nitric oxide synthase (NOS2), an enzyme essential to control chronic *M. tuberculosis* infection. NOS2-deficient mice lack nitric oxide synthase and succumb to chronic *M. tuberculosis* infection within months, whereas wild-type C57BL/6 mice can survive with chronic infection indefinitely despite disseminated disease and high bacterial burden (38, 39). The experimental schematic of infection is presented in Fig. 5a. We first confirmed that P2C/5-OP-RU treatment induced equivalent enrichment of MAIT cells in the lungs in both WT and NOS2-deficient strains in the absence of infection (Fig. 5b). MAIT cell enrichment in the spleen was decreased in NOS2-deficient mice (Fig. 5c). We then infected WT and NOS2-deficient mice with a standard LD *M. tuberculosis* inoculum targeting 50 to 150 CFU/lung and evaluated immunologic and bacteriologic outcomes 21 days postinfection as well as mortality. Absolute numbers of MAIT cells were enriched in the lungs of P2C/5-OP-RU-primed mice in both strains (Fig. 5d). We observed no significant difference in *M. tuberculosis* antigen-specific T cells between treatment groups (Fig. 5e and f). As expected, NOS2-deficient mice had approximately 10-fold higher bacterial loads than WT mice, but no significant difference was observed in lung bacterial loads after P2C/5-OP-RU priming (Fig. 5g). Although there was a trend toward enhanced spleen bacterial control in P2C/5-OP-RU-treated NOS2-deficient mice, this did not reach statistical significance (693,000 versus 149,000, $P = 0.18$) (Fig. 5h). All 20 NOS2-deficient mice died or were euthanized as a humane endpoint by ~11 weeks after infection, while 9/10 WT mice survived. We observed a longer median survival of P2C/5-OP-RU-treated NOS2-deficient mice relative to those treated with P2C alone, but this trend also did not reach statistical significance (72.5 versus 56.5 days; $P = 0.18$) (Fig. 5i).

DISCUSSION

Emerging evidence from murine infection models of *Francisella* and *Legionella* spp. support a protective role for MAIT cells against intracellular pulmonary bacterial pathogens (10, 30, 32, 33). Importantly, MAIT cell priming prior to murine *Legionella longbeachae* infection significantly attenuated bacterial load and was dependent on MR1, granulocyte-macrophage colony-stimulating factor (GM-CSF), and IFN-γ but not on perforin, interleukin 17A (IL-17A), or tumor necrosis factor alpha (TNF-α) (30, 32).

In contrast to these studies, prior literature indicates that MAIT cells undergo limited expansion after pulmonary *M. tuberculosis* infection in mice and macaques (23–25). This is consistent with our findings: we observed initial MAIT cell depletion from the inguinal lymph node, spleen, and lung at day 7 postinfection, likely explained by rapid MAIT cell

FIG 3 Legend (Continued)
cell priming prior to *M. tuberculosis* (*Mtb*) infection. (b) Mean percent MAIT cells of T cells ± SEMs and mean MAIT cell absolute numbers ± SEMs in the lung over time in uninfected and infected mice receiving intranasal inoculation with 16.7 μg of P2C alone or P2C/2 mM 5-OP-RU costimulation. Time zero is the time of aerosol challenge in infected mice. (c) MAIT cell intracellular staining in mouse lungs from day 2 and 7 postinfection, measured by the mean percent difference between 5-OP-RU and resting conditions ± SEMs after 15 h of *in vitro* restimulation. Mean percent ESAT-6- or TB10.4-specific T cells ± SEMs in the lung (d) or spleen (e) at day 29 postinfection. blue, P2C; red, P2C/5-OP-RU. Same legend applies to panels e to g. (f and g) *M. tuberculosis* CFU in the lung (f) and spleen (g) over time. $n = 3$ to 8 mice/group. Data in this figure are representative of three independent experiments. Statistical analyses were performed using unpaired *t* tests. *, $P < 0.05$; ****, $P < 0.0001$; GZMB, granzyme B.

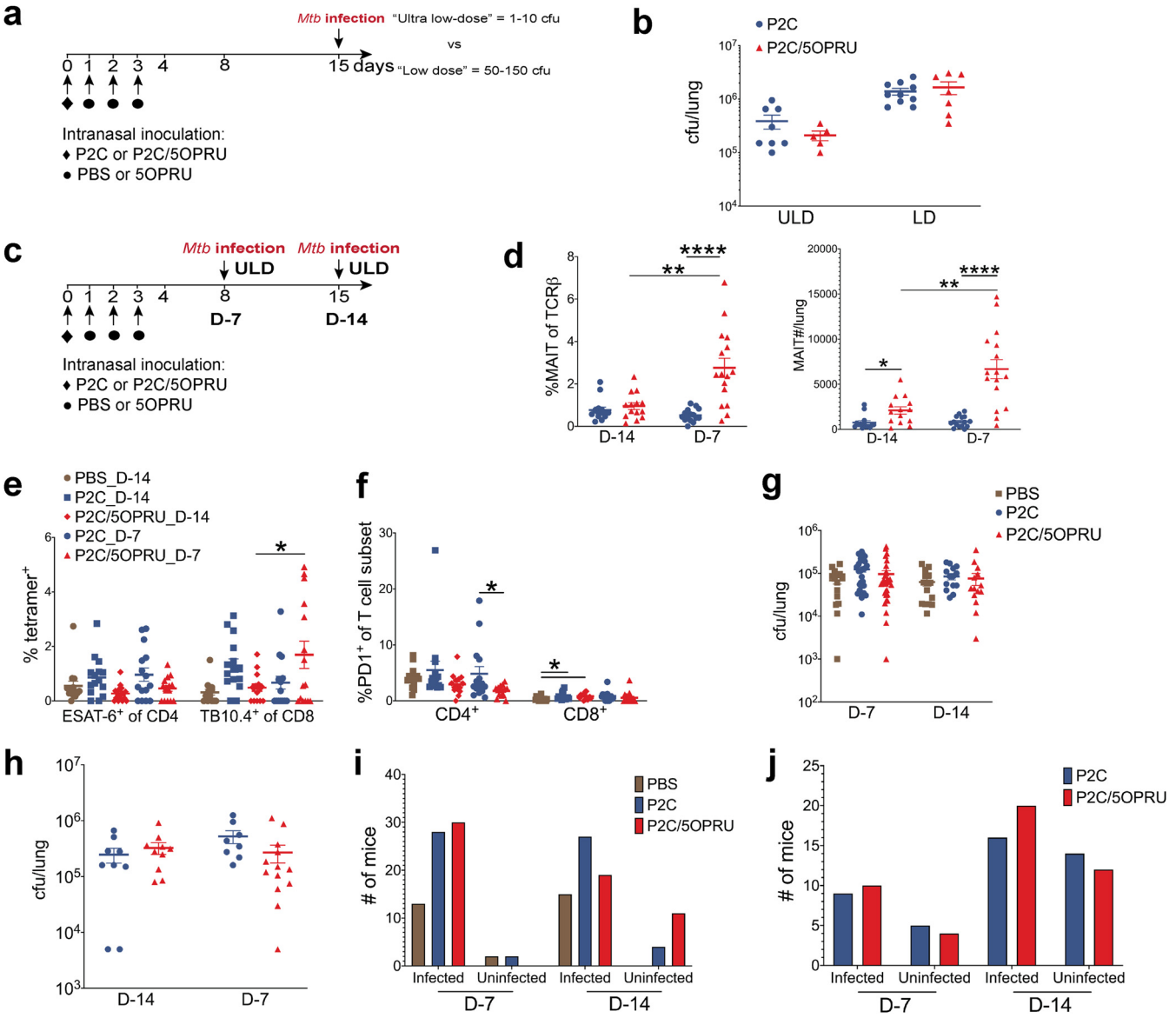

FIG 4 Variation of *M. tuberculosis* inoculum or infection schedule did not attenuate *M. tuberculosis* infection in MAIT cell-primed mice. (a) Experimental schematic of ultralow-dose (ULD) versus low-dose (LD) *M. tuberculosis* infection after MAIT cell priming. (b) Mean *M. tuberculosis* CFU ± SEMs in the lung at 21 days postinfection stratified by inoculum. (c) Experimental schematic of two infection schedules. (d) Mean percent MAIT cells of T cells ± SEMs and mean MAIT cell absolute numbers ± SEMs in the lung 24 days postinfection stratified by infection schedule. (e) Mean percent ESAT-6 or TB10.4$^+$ T cells of CD4$^+$ or CD8$^+$ T cells ± SEMs 24 days postinfection under different infection schedules. (f) Mean percent PD-1$^+$ of CD4$^+$ or CD8$^+$ T cells ± SEMs 24 days postinfection. (g and h) Mean *M. tuberculosis* CFU ± SEMs at 14 (g) and 24 (h) days postinfection using two infection schedules. Numbers of infected and uninfected mice per treatment group after aerosol challenge with ULD inoculum at 14 (i) and 24 (j) days postinfection. Data in panels b and d to f represent one independent experiment. Data from panels g and i and from panels h and j represent 3 and 2 independent experiments, respectively. $n = 15$ to 30 mice/group. Statistical analyses were performed using unpaired *t* tests. *, $P < 0.05$; **, $P < 0.005$; ****, $P < 0.0001$.

TCR downregulation and apoptosis following acute exposure (3, 26, 40–42). After 21 days, *M. tuberculosis* induced only a mild MAIT cell expansion in the lung and mediastinal lymph node when antigen-specific conventional T cells were robustly proliferating (43). Our data, together with previously published observations in humans (18) and animal models (24, 25), suggest that early MAIT cell responses may be suppressed by *M. tuberculosis* infection.

Despite this limited expansion, several pieces of evidence suggested that selective MAIT cell priming would enhance antimycobacterial activity. *In vitro*, MAIT cells can inhibit *Mycobacterium bovis* BCG growth in infected murine macrophages (44). *In vivo*, transgenic mice overexpressing the murine MAIT cell Vα19 TCR demonstrate decreased

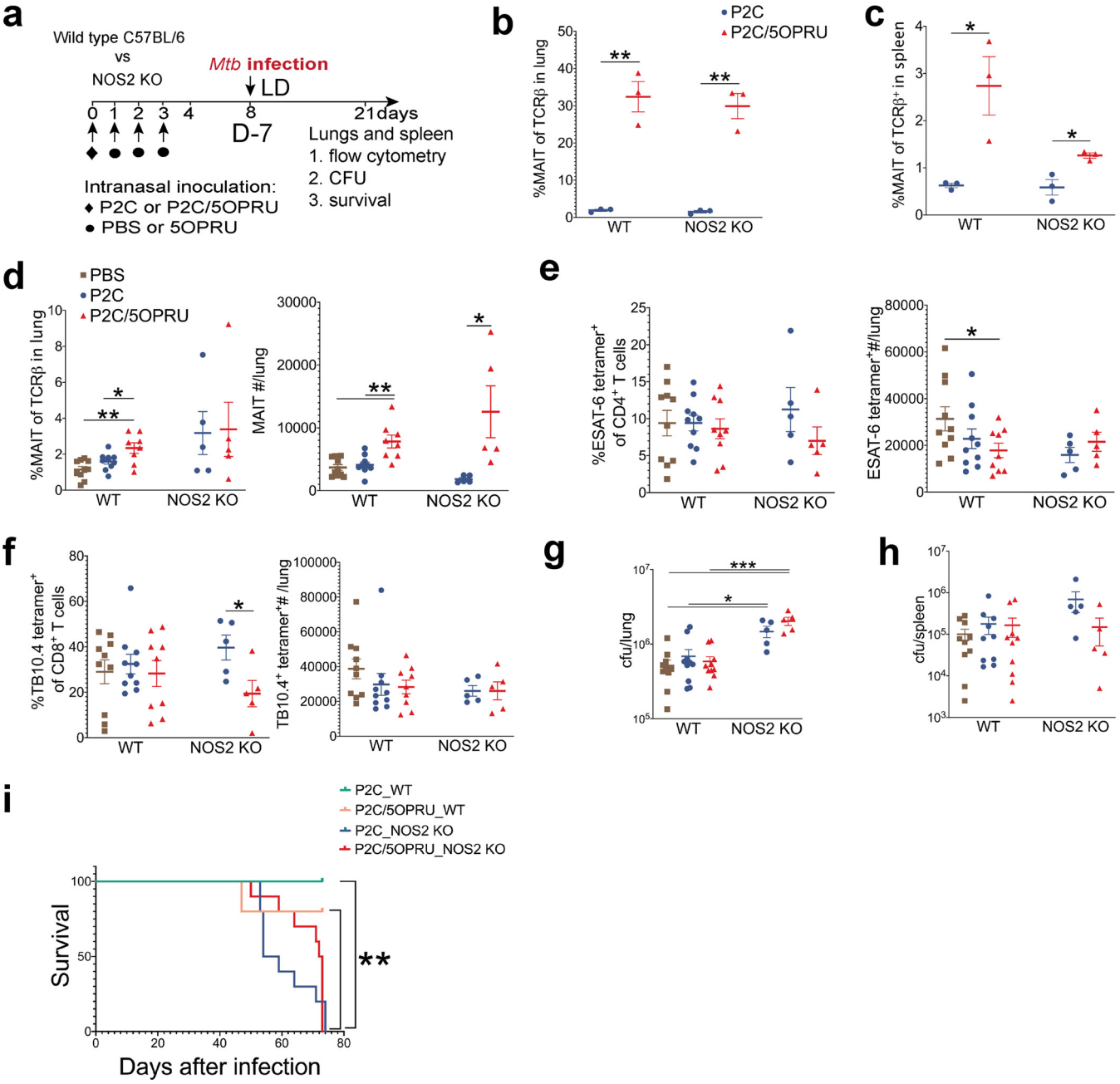

FIG 5 MAIT cell priming does not rescue hypersusceptible NOS2-deficient mice from lethal infection. (a) Experimental schematic of MAIT cell priming prior to *M. tuberculosis* infection of wild-type (WT) C57BL/6 or nitric oxide synthase 2 (NOS2) knockout (KO) mice. Mean percent MAIT cells of T cells ± SEMs in the lungs (b) and spleens (c) of uninfected mice 7 days after receiving intranasal priming. $n = 3$ mice/group. (d) Mean percent MAIT cells of T cells ± SEMs and mean MAIT cell absolute numbers ± SEM in lungs 21 days after infection. (e and f) Mean percent ESAT-6 (e) or TB10.4 (f) antigen-specific T cells of $CD4^+$ or $CD8^+$ T cells, respectively, ± SEMs 21 days postinfection. Mean *M. tuberculosis* CFU ± SEMs in WT and NOS2 KO mice in lungs (g) and spleens (h) 21 days postinfection. $n = 5$ to 10 mice/group in panels d to h. (i) Survival of *M. tuberculosis*-infected WT ($n = 5$ mice/group) and NOS2 KO mice ($n = 10$ mice/group). All data in this figure represent one independent experiment. Statistical analyses were performed using unpaired *t* tests in all panels except for panel g, where a log rank test was used. *, $P < 0.05$; **, $P < 0.005$; ***, $P < 0.0005$.

M. tuberculosis lung burden compared to that in wild-type mice (23). In BCG-vaccinated macaques and humans, MAIT cells demonstrate rapid expansion and enhanced IFN-γ production (14, 34, 45). In healthy household contacts of TB patients, MAIT cells demonstrate enhanced function in highly exposed donors who remain uninfected (3, 15). Taken together, these data support the hypothesis that direct targeting of MAIT cells prior to *M. tuberculosis* challenge may attenuate the course of infection.

We hypothesized that the recruitment of MAIT cells to the lung prior to aerosol *M. tuberculosis* challenge could enhance their cytotoxic and helper activity during infection and confer protective immunity. However, our results convincingly demonstrate that intrapulmonary MAIT cell activation and expansion prior to *M. tuberculosis* challenge is not sufficient to attenuate bacterial load. Furthermore, we show that while MAIT cells are activated and expand early in P2C/5-OP-RU-treated infected mice, they are subsequently depleted. These results mirror observations of peripheral MAIT cell depletion and upregulation of exhaustion markers during active TB infection in humans (12, 13, 17). We also highlight that neither decreasing *M. tuberculosis* inoculum nor the time between priming and infection impacted bacteriologic outcomes. Overall, our study findings are consistent with early MAIT cell activation and expansion with priming prior to *M. tuberculosis* infection, but no protection against murine aerosol *M. tuberculosis* infection.

Our results are consistent with recent work in *M. tuberculosis*-infected macaques demonstrating mild enrichment of MAIT cells in bronchoalveolar fluid by 21 days postinfection, a time point when *M. tuberculosis* antigen-specific T cells are more robustly expanding in the lung (24). In that study, MAIT cells were also sparsely detected in granulomas and did not correlate with *M. tuberculosis* bacterial load, suggesting a limited role for MAIT cell immunity against *M. tuberculosis* in the nonhuman primate model.

Importantly, our results strikingly contrast with MAIT cell priming efficacy in a *Legionella* model (30, 32) and prompt further inquiry into why MAIT cells are unable to control *M. tuberculosis* infection despite enhanced numbers and effector functions. Specifically, the efficacy of targeted MAIT cell immune therapy may depend upon the capacity of the pathogen itself to induce MAIT cell proliferation as seen with *Francisella* (33) or *Legionella* spp. (30, 32), a feature that may reflect the availability of appropriate MR1 presented ligand.

One technical difference between infection models is that sublethal doses of *Legionella longbeachae* or *Francisella* live vaccine strain (LVS) lead to attenuated infection and eventual clearance by wild-type mice, even without P2C/5-OP-RU priming (30, 33). In contrast, we show that even an ultralow-dose *M. tuberculosis* infection targeting 1 to 10 CFU/mouse results in chronic infection with high bacterial burdens that cannot be cleared without antibiotics (46, 47). However, we do not believe this alone can explain the disparate MAIT cell vaccination efficacies between models, since protection conferred by MAIT cell priming against *Legionella* was observed early after infectious challenge, at the peak of the bacterial burden.

The microbial mechanisms underlying attenuated MAIT cell responses against *M. tuberculosis* infection in animal models remain poorly understood. We speculate that MAIT cells are inefficiently activated by *M. tuberculosis*-derived MR1 ligands during *in vivo* infection. One reason may be that *M. tuberculosis* does not provide sufficient quantities of activating MR1 ligands to the host, due to lower replication rates (48, 49), resulting in inefficient MR1 trafficking and presentation *in vivo* (50). Additionally, *M. tuberculosis* could produce inhibitory MR1 ligands that suppress MAIT cell activation. Recent studies suggest that mycobacterium-derived MR1 ligand compositions differ from those of other bacterial species (50, 51). Mass spectrometry of eluates from human tetramers bearing ligands from the evolutionarily related *Mycobacterium smegmatis* detected decreased MR1-activating ligands rRL-6-CH_2OH/5-OP-RU and RL-6-M27-OH relative to those from *Escherichia coli* (51). Moreover, MR1 inhibitory ligands, including riboflavin itself and 7,8-didemethyl-8-hydroxy-5-deazariboflavin (FO), were only detected in *M. smegmatis* tetramers but not in *E. coli* (51). Importantly, these differences translated into decreased IFN-γ responses of MR1-reactive T cell clones to *M. smegmatis*-derived ligands compared to those from *E. coli*. Taken together, these data raise the possibility that *M. tuberculosis*-derived MR1 ligands may induce a net inhibitory effect on MR1 signaling and suppress MAIT cell activation, despite efficient 5-OP-RU priming prior to infection.

Our results also contrast with the immunotherapeutic efficacy of the other main *M. tuberculosis*-reactive innate-like T cell subset: Vγ9δ2 T cells that respond to *M. tuberculosis*-derived phosphoantigens in primates (3, 52, 53). Pulmonary *M. tuberculosis* infection alone induces robust Vγ9δ2 T cell proliferation in macaques (54), and intrapulmonary phosphoantigen/IL-2 priming prior to *M. tuberculosis* challenge enhanced the recruitment of *M. tuberculosis* antigen-specific T cells to the lung and attenuated the bacterial load (55). In contrast, P2C/5-OP-RU priming of MAIT cells neither attenuated infection nor significantly enhanced recruitment of *M. tuberculosis* antigen-specific T cells.

Emerging data would suggest that adjunctive cytokine stimulation may enhance MAIT cell activity against mycobacterial infection. MAIT cell responses from BCG-revaccinated human donors were more dependent on IL-12/IL-18 signaling than on MR1 (14). In a separate study, enhanced MAIT cell responses from human tuberculous pleural effusions were also found to be cytokine dependent (21). Importantly, IL-23 was shown to be necessary for MAIT cell expansion after murine pulmonary *S*. Typhimurium infection (32). In this same study, administration of synthetic 5-OP-RU plus IL-23 costimulation enhanced antimicrobial responses against murine *Legionella* similarly to TLR2/6 ligand plus 5-OP-RU costimulation previously reported (30, 32). We hypothesize that MAIT cell protective immunity during *M. tuberculosis* infection may require additional activating signals not acquired by P2C plus 5-OP-RU priming alone. Future studies should test additional MAIT cell priming approaches against *M. tuberculosis*, including cytokine costimulation with IL-12/-18/-23.

In sum, we demonstrate that intranasal 5-OP-RU and TLR2/6 costimulation prior to aerosol *M. tuberculosis* challenge in mice enhances MAIT cell activation and expansion in the lung but is not sufficient to attenuate infection. Our findings stand in contrast with the efficacy of MAIT cell priming observed in a *Legionella* infection model, indicating that the translational potential of MAIT cell priming is likely pathogen specific. These results will make important contributions to future studies targeting MAIT cells as antimicrobial immunotherapy.

MATERIALS AND METHODS

Animals and *M. tuberculosis* infections. Wild-type C57BL/6 mice were obtained from Jackson Laboratories (C57BL/6J, number 000664) (Fig. 1) or Taconic Laboratories (B6NTac) (Fig. 2 and 5). Additional wild-type C57BL/6 mice were obtained from Envigo (C57BL/6JRccHsd) and Charles River (C57BL/6NCrl, number 027) Laboratories (see Fig. S2 in the supplemental material). NOS2-deficient mice (B6.129P2-Nos2^{tm1Lau}/J number 002609) were obtained from Jackson Laboratories (Fig. 5). Female mice were used during *M. tuberculosis* infection due to the extended duration of cohousing. All mice were housed in an animal biological safety level 3 (ABSL3) vivarium which is fully accredited by AAALAC International. For *M. tuberculosis* infection, animals were infected in an aerosol chamber with either standard low-dose inoculum of log-phase Erdman strain *M. tuberculosis* at a concentration of 8×10^6/ml in 5 ml of deionized water or ultralow-dose inoculum at a concentration of 6×10^5/ml in 5 ml of deionized water.

Animals were contained in ABSL3 biocontainment racks and were given food and water *ad libitum*. All housing of and procedures involving animals were according to the Animal Welfare Act, the guide for the care and use of laboratory animals, the AVMA guidelines on euthanasia, and other federal statutes. All procedures were approved by the MSKCC Animal Care and Use Committee under approved animal study proposal 01-11-030.

MAIT cell priming by intranasal inoculation. Mice were intranasally inoculated with 16.7 μg Pam2Cys (Invivogen) or Pam2Cys plus 2 mM 5-A-RU (Aubé laboratory) plus 50 μM methylglyoxal (Sigma) in 100 μl on day 0, followed by 1$\times$ phosphate-buffered saline (PBS) or 2 mM 5-ARU/50 μM methylglyoxal on days 1, 2, and either 3 or 4. 5-A-RU was synthesized as previously described (26), resuspended in sterile water, and cryopreserved in 12.5 mM aliquots. 5-A-RU was thawed as needed and directly added to methylglyoxal at the time of intranasal inoculation.

Processing of tissues, *in vitro* stimulations, and flow cytometry. Tissues were resected and underwent 3 min of bead beating at speed 6 using 10 2.0-mm zirconium oxide beads/sample in 1 ml (lungs and spleen) or 5 beads/sample in 0.5 ml of RPMI-10% fetal bovine serum (FBS) in a Bullet blender (Next Advance). Homogenized tissues were passed through 100-μm strainers and centrifuged at 400 $\times$ *g* for 3 min, and the supernatant was decanted. The tissues were then incubated for 5 min in RBC lysis buffer (Gibco ACK Lysing buffer) prior to final washing and *in vitro* assays or flow cytometry.

Lungs and spleen for *M. tuberculosis* culture were homogenized by 4 min of bead beating at speed 8 in 1 ml of 1$\times$ PBS-0.05% Tween 80. All CFU measurements were serial dilutions on 7H10 Middlebrook agar plates (Difco) supplemented with oleic acid-albumin-dextrose-catalase (OADC).

For *in vitro* restimulation assays, single cell suspensions of lung were incubated for 15 h in RPMI-10% FBS alone or 2 μM 5-A-RU added to 50 μM methylglyoxal in 96-well plates incubated at 37°C and 5% CO_2. Brefeldin A was added during the last 2 h of stimulation.

Prior to fluorescent staining, FcγR blockade (CD16/CD32; clone 93) was performed for 15 min at room temperature in 50 μl. Extracellular staining was performed for 15 min at room temperature in 50 μl, and intracellular staining was performed after 40 min of permeabilization/fixation at 4°C. For ESAT-6 and TB10.4 tetramers, cells were incubated with tetramers alone first for 1 h at 37°C prior to staining with other antibodies. Intracellular antibody cocktails were incubated for 1 h at 4°C in 50 μl. We used MR1-5-OP-RU tetramers to identify MAIT cells and MR1-6FP tetramers as staining controls. ESAT-6 and TB10.4 tetramers were employed to identify *M. tuberculosis* antigen-specific T cells. All tetramers were produced by the NIAID tetramer core facility (Emory University, Atlanta, GA) (26). We used the following fluorochrome-labeled antibodies with their respective clones in parentheses: TCRβ (H57-597), FoxP3 (FJK-16S), MHC II (M5/114.15.2), CD25 (PC61), CD4 (GK1.5), CD69 (H1.2F3), IFN-γ (XMG1.2), IL-17A (TC11-18H10), F4/80 (BM8), CD45R/B220 (RA3-6B2), CD44 (IM7), granzyme B (QA16AA02), CD90.2 (30-H12), TCR$\gamma\delta$ (GL3), CD19 (6D5), CD8 (53-6.7), PD-1 (29F.1A12), and (NK1.1 PK136). All *M. tuberculosis*-infected tissues were fixed in 2% formaldehyde for 2 h prior to acquiring on a BD Fortessa instrument. Absolute numbers were normalized using Precision Count Beads (BioLegend). Flow cytometry data were analyzed using FCS express software (v. 7; De Novo Software, Pasadena, CA).

Statistical analysis. All statistical analyses were performed in Prism (v. 8; GraphPad Software, La Jolla, CA). Two-tailed unpaired *t* tests with significance at a *P* value of <0.05 were used to compare immunologic or CFU differences between P2C/5-OP-RU or P2C treatment groups. A log rank test with significance at a *P* value of <0.05 was used to compare survival of NOS2-deficient mice.

SUPPLEMENTAL MATERIAL

Supplemental material is available online only.

SUPPLEMENTAL FILE 1, PDF file, 2.6 MB.

ACKNOWLEDGMENTS

We thank Ashutosh Chaudhry and Alexander Rudensky, Sloan Kettering Institute, MSKCC, for valuable advice and discussions while conducting these experiments. We thank Kevin Urdahl, University of Washington, for his guidance regarding the ultralow-dose inoculum in our *M. tuberculosis* aerosol infection model. We also thank Matthew Adamow and Phillip Wong of the MSKCC immune monitoring core facility as well as Rui Gardner, Kathy Daniels, Mark Kweens, and Fang Fang of the MSKCC flow cytometry core facility for their expert consultation. MR1, ESAT-6, and TB10.4 tetramers were produced by the NIH tetramer core facility.

This work was supported by the Tri-I TBRU, part of the TBRU Network (U19 AI111143), and P30 CA008748. C.K.V. was supported by NIAID K08AI132739.

M.S.G. has received consulting fees and holds equity in Vedanta Biosciences, has received consulting fees from Takeda, and is on the scientific advisory board of PRL-NYC.

C.K.V. and M.S.G. conceived of the study. C.K.V., O.L., and M.S. conducted the experiments. K.L. and J.A. synthesized 5-A-RU. C.K.V. and M.S.G. analyzed and interpreted the data and wrote the manuscript with input from all the authors.

REFERENCES

1. Treiner E, Duban L, Bahram S, Radosavljevic M, Wanner V, Tilloy F, Affaticati P, Gilfillan S, Lantz O. 2003. Selection of evolutionarily conserved mucosal-associated invariant T cells by MR1. Nature 422:164–169. https://doi.org/10.1038/nature01433.
2. Godfrey DI, Koay HF, McCluskey J, Gherardin NA. 2019. The biology and functional importance of MAIT cells. Nat Immunol 20:1110–1128. https://doi.org/10.1038/s41590-019-0444-8.
3. Vorkas CK, Wipperman MF, Li K, Bean J, Bhattarai SK, Adamow M, Wong P, Aube J, Juste MAJ, Bucci V, Fitzgerald DW, Glickman MS. 2018. Mucosal-associated invariant and $\gamma\delta$ T cell subsets respond to initial *Mycobacterium tuberculosis* infection. JCI Insight 3:e121899. https://doi.org/10.1172/jci.insight.121899.
4. Lamichhane R, Schneider M, de la Harpe SM, Harrop TWR, Hannaway RF, Dearden PK, Kirman JR, Tyndall JDA, Vernall AJ, Ussher JE. 2019. TCR- or cytokine-activated $CD8^+$ mucosal-associated invariant T cells are rapid polyfunctional effectors that can coordinate immune responses. Cell Rep 28:3061.e5–3076.e5. https://doi.org/10.1016/j.celrep.2019.08.054.
5. Le Bourhis L, Dusseaux M, Bohineust A, Bessoles S, Martin E, Premel V, Coré M, Sleurs D, Serriari NE, Treiner E, Hivroz C, Sansonetti P, Gougeon ML, Soudais C, Lantz O. 2013. MAIT cells detect and efficiently lyse bacterially-infected epithelial cells. PLoS Pathog 9:e1003681. https://doi.org/10.1371/journal.ppat.1003681.
6. Kurioka A, Ussher JE, Cosgrove C, Clough C, Fergusson JR, Smith K, Kang YH, Walker LJ, Hansen TH, Willberg CB, Klenerman P. 2015. MAIT cells are licensed through granzyme exchange to kill bacterially sensitized targets. Mucosal Immunol 8:429–440. https://doi.org/10.1038/mi.2014.81.
7. Lu B, Liu M, Wang J, Fan H, Yang D, Zhang L, Gu X, Nie J, Chen Z, Corbett AJ, Zhan MJ, Zhang S, Bryant VL, Lew AM, McCluskey J, Luo HB, Cui J, Zhang Y, Zhan Y, Lu G. 2020. IL-17 production by tissue-resident MAIT cells is locally induced in children with pneumonia. Mucosal Immunol 13:824–835. https://doi.org/10.1038/s41385-020-0273-y.
8. Rahman MA, Ko EJ, Bhuyan F, Enyindah-Asonye G, Hunegnaw R, Helmold Hait S, Hogge CJ, Venzon DJ, Hoang T, Robert-Guroff M. 2020. Mucosal-associated invariant T (MAIT) cells provide B-cell help in vaccinated and subsequently SIV-infected. Sci Rep 10:10060. https://doi.org/10.1038/s41598-020-66964-0.

9. Bennett MS, Trivedi S, Iyer AS, Hale JS, Leung DT. 2017. Human mucosal-associated invariant T (MAIT) cells possess capacity for B cell help. J Leukoc Biol 102:1261–1269. https://doi.org/10.1189/jlb.4A0317-116R.
10. Downey AM, Kapłonek P, Seeberger PH. 2019. MAIT cells as attractive vaccine targets. FEBS Lett 593:1627–1640. https://doi.org/10.1002/1873-3468.13488.
11. Godfrey DI, Le Nours J, Andrews DM, Uldrich AP, Rossjohn J. 2018. Unconventional T cell targets for cancer immunotherapy. Immunity 48:453–473. https://doi.org/10.1016/j.immuni.2018.03.009.
12. Jiang J, Cao Z, Qu J, Liu H, Han H, Cheng X. 2020. PD-1-expressing MAIT cells from patients with tuberculosis exhibit elevated production of CXCL13. Scand J Immunol 91:e12858. https://doi.org/10.1111/sji.12858.
13. Jiang J, Wang X, An H, Yang B, Cao Z, Liu Y, Su J, Zhai F, Wang R, Zhang G, Cheng X. 2014. Mucosal-associated invariant T-cell function is modulated by programmed death-1 signaling in patients with active tuberculosis. Am J Respir Crit Care Med 190:140630082918004–140630082918039. https://doi.org/10.1164/rccm.201401-0106OC.
14. Suliman S, Murphy M, Musvosvi M, Gela A, Meermeier EW, Geldenhuys H, Hopley C, Toefy A, Bilek N, Veldsman A, Hanekom WA, Johnson JL, Boom WH, Obermoser G, Huang H, Hatherill M, Lewinsohn DM, Nemes E, Scriba TJ. 2019. MR1-independent activation of human mucosal-associated invariant T cells by mycobacteria. J Immunol 203:2917–2927. https://doi.org/10.4049/jimmunol.1900674.
15. Coulter F, Parrish A, Manning D, Kampmann B, Mendy J, Garand M, Lewinsohn DM, Riley EM, Sutherland JS. 2017. IL-17 production from T helper 17, mucosal-associated invariant T, and $\gamma\delta$ cells in tuberculosis infection and disease. Front Immunol 8:1252. https://doi.org/10.3389/fimmu.2017.01252.
16. Malka-Ruimy C, Ben Youssef G, Lambert M, Tourret M, Ghazarian L, Faye A, Caillat-Zucman S, Houdouin V. 2019. Mucosal-associated invariant T cell levels are reduced in the peripheral blood and lungs of children with active pulmonary tuberculosis. Front Immunol 10:206. https://doi.org/10.3389/fimmu.2019.00206.
17. Gold MC, Cerri S, Smyk-Pearson S, Cansler ME, Vogt TM, Delepine J, Winata E, Swarbrick GM, Chua WJ, Yu YY, Lantz O, Cook MS, Null MD, Jacoby DB, Harriff MJ, Lewinsohn DA, Hansen TH, Lewinsohn DM. 2010. Human mucosal associated invariant T cells detect bacterially infected cells. PLoS Biol 8:e1000407. https://doi.org/10.1371/journal.pbio.1000407.
18. Jiang J, Yang B, An H, Wang X, Liu Y, Cao Z, Zhai F, Wang R, Cao Y, Cheng X. 2016. Mucosal-associated invariant T cells from patients with tuberculosis exhibit impaired immune response. J Infect 72:338–352. https://doi.org/10.1016/j.jinf.2015.11.010.
19. Le Bourhis L, Martin E, Peguillet I, Guihot A, Froux N, Core M, Levy E, Dusseaux M, Meyssonnier V, Premel V, Ngo C, Riteau B, Duban L, Robert D, Huang S, Rottman M, Soudais C, Lantz O. 2010. Antimicrobial activity of mucosal-associated invariant T cells. Nat Immunol 11:701–708. https://doi.org/10.1038/ni.1890.
20. Kwon YS, Cho YN, Kim MJ, Jin HM, Jung HJ, Kang JH, Park KJ, Kim TJ, Kee HJ, Kim N, Kee SJ, Park YW. 2015. Mucosal-associated invariant T cells are numerically and functionally deficient in patients with mycobacterial infection and reflect disease activity. Tuberculosis (Edinb) 95:267–274. https://doi.org/10.1016/j.tube.2015.03.004.
21. Jiang J, Chen X, An H, Yang B, Zhang F, Cheng X. 2016. Enhanced immune response of MAIT cells in tuberculous pleural effusions depends on cytokine signaling. Sci Rep 6:32320. https://doi.org/10.1038/srep32320.
22. Wong EB, Gold MC, Meermeier EW, Xulu BZ, Khuzwayo S, Sullivan ZA, Mahyari E, Rogers Z, Kloverpris H, Sharma PK, Worley AH, Lalloo U, Baijnath P, Ambaram A, Naidoo L, Suleman M, Madansein R, McLaren JE, Ladell K, Miners KL, Price DA, Behar SM, Nielsen M, Kasprowicz VO, Leslie A, Bishai WR, Ndung'u T, Lewinsohn DM. 2019. TRAV1-2^{+} CD8^{+} T-cells including oligoconal expansions of MAIT cells are enriched in the airways in human tuberculosis. Commun Biol 2:203. https://doi.org/10.1038/s42003-019-0442-2.
23. Sakala IG, Kjer-Nielsen L, Eickhoff CS, Wang X, Blazevic A, Liu L, Fairlie DP, Rossjohn J, McCluskey J, Fremont DH, Hansen TH, Hoft DF. 2015. Functional heterogeneity and antimycobacterial effects of mouse mucosal-associated invariant T cells specific for riboflavin metabolites. J Immunol 195:587–601. https://doi.org/10.4049/jimmunol.1402545.
24. Kauffman KD, Sallin MA, Hoft SG, Sakai S, Moore R, Wilder-Kofie T, Moore IN, Sette A, Arlehamn CSL, Barber DL. 2018. Limited pulmonary mucosal-associated invariant T cell accumulation and activation during *Mycobacterium tuberculosis* infection in rhesus macaques. Infect Immun 86:e00431-18. https://doi.org/10.1128/IAI.00431-18.
25. Bucsan AN, Rout N, Foreman TW, Khader SA, Rengarajan J, Kaushal D. 2019. Mucosal-activated invariant T cells do not exhibit significant lung recruitment and proliferation profiles in macaques in response to infection with *Mycobacterium tuberculosis* CDC1551. Tuberculosis (Edinb) 116:S11–S18. https://doi.org/10.1016/j.tube.2019.04.006.
26. Li K, Vorkas CK, Chaudhry A, Bell DL, Willis RA, Rudensky A, Altman JD, Glickman MS, Aube J. 2018. Synthesis, stabilization, and characterization of the MR1 ligand precursor 5-amino-6-D-ribitylaminouracil (5-A-RU). PLoS One 13:e0191837. https://doi.org/10.1371/journal.pone.0191837.
27. Cui Y, Franciszkiewicz K, Mburu YK, Mondot S, Le Bourhis L, Premel V, Martin E, Kachaner A, Duban L, Ingersoll MA, Rabot S, Jaubert J, De Villartay JP, Soudais C, Lantz O. 2015. Mucosal-associated invariant T cell-rich congenic mouse strain allows functional evaluation. J Clin Invest 125:4171–4185. https://doi.org/10.1172/JCI82424.
28. Legoux F, Bellet D, Daviaud C, El Morr Y, Darbois A, Niort K, Procopio E, Salou M, Gilet J, Ryffel B, Balvay A, Foussier A, Sarkis M, El Marjou A, Schmidt F, Rabot S, Lantz O. 2019. Microbial metabolites control the thymic development of mucosal-associated invariant T cells. Science 366:494–499. https://doi.org/10.1126/science.aaw2719.
29. Chen Z, Wang H, D 'souza C, Sun S, Kostenko L, Eckle S, Meehan B, Jackson D, Strugnell R, Cao H, Wang N, Fairlie D, Liu L, Godfrey D, Rossjohn J, Mccluskey J, Corbett A. 2017. Mucosal-associated invariant T-cell activation and accumulation after *in vivo* infection depends on microbial riboflavin synthesis and co-stimulatory signals. Mucosal Immunol 10:58–68. https://doi.org/10.1038/mi.2016.39.
30. Wang H, D'Souza C, Lim XY, Kostenko L, Pediongco TJ, Eckle SBG, Meehan BS, Shi M, Wang N, Li S, Liu L, Mak JYW, Fairlie DP, Iwakura Y, Gunnersen JM, Stent AW, Godfrey DI, Rossjohn J, Westall GP, Kjer-Nielsen L, Strugnell RA, McCluskey J, Corbett AJ, Hinks TSC, Chen Z. 2018. MAIT cells protect against pulmonary *Legionella longbeachae* infection. Nat Commun 9:3350. https://doi.org/10.1038/s41467-018-05202-8.
31. Ben Youssef G, Tourret M, Salou M, Ghazarian L, Houdouin V, Mondot S, Mburu Y, Lambert M, Azarnoush S, Diana JS, Virlouvet AL, Peuchmaur M, Schmitz T, Dalle JH, Lantz O, Biran V, Caillat-Zucman S. 2018. Ontogeny of human mucosal-associated invariant T cells and related T cell subsets. J Exp Med 215:459–479. https://doi.org/10.1084/jem.20171739.
32. Wang H, Kjer-Nielsen L, Shi M, D'Souza C, Pediongco TJ, Cao H, Kostenko L, Lim XY, Eckle SBG, Meehan BS, Zhu T, Wang B, Zhao Z, Mak JYW, Fairlie DP, Teng MWL, Rossjohn J, Yu D, de St Groth BF, Lovrecz G, Lu L, McCluskey J, Strugnell RA, Corbett AJ, Chen Z. 2019. IL-23 costimulates antigen-specific MAIT cell activation and enables vaccination against bacterial infection. Sci Immunol 4:eaaw0402. https://doi.org/10.1126/sciimmunol.aaw0402.
33. Meierovics A, Yankelevich WJ, Cowley SC. 2013. MAIT cells are critical for optimal mucosal immune responses during *in vivo* pulmonary bacterial infection. Proc Natl Acad Sci U S A 110:E3119–28. https://doi.org/10.1073/pnas.1302799110.
34. Greene JM, Dash P, Roy S, McMurtrey C, Awad W, Reed JS, Hammond KB, Abdulhaqq S, Wu HL, Burwitz BJ, Roth BF, Morrow DW, Ford JC, Xu G, Bae JY, Crank H, Legasse AW, Dang TH, Greenaway HY, Kurniawan M, Gold MC, Harriff MJ, Lewinsohn DA, Park BS, Axthelm MK, Stanton JJ, Hansen SG, Picker LJ, Venturi V, Hildebrand W, Thomas PG, Lewinsohn DM, Adams EJ, Sacha JB. 2017. MR1-restricted mucosal-associated invariant T (MAIT) cells respond to mycobacterial vaccination and infection in nonhuman primates. Mucosal Immunol 10:802–813. https://doi.org/10.1038/mi.2016.91.
35. Napier RJ, Adams EJ, Gold MC, Lewinsohn DM. 2015. The role of mucosal associated invariant T cells in antimicrobial immunity. Front Immunol 6:344. https://doi.org/10.3389/fimmu.2015.00344.
36. Shiloh MU. 2016. Mechanisms of mycobacterial transmission: how does *Mycobacterium tuberculosis* enter and escape from the human host. Future Microbiol 11:1503–1506. https://doi.org/10.2217/fmb-2016-0185.
37. Hoal-van Helden EG, Hon D, Lewis LA, Beyers N, van Helden PD. 2001. Mycobacterial growth in human macrophages: variation according to donor, inoculum and bacterial strain. Cell Biol Int 25:71–81. https://doi.org/10.1006/cbir.2000.0679.
38. MacMicking JD, North RJ, LaCourse R, Mudgett JS, Shah SK, Nathan CF. 1997. Identification of nitric oxide synthase as a protective locus against tuberculosis. Proc Natl Acad Sci U S A 94:5243–5248. https://doi.org/10.1073/pnas.94.10.5243.
39. Cooper AM, Pearl JE, Brooks JV, Ehlers S, Orme IM. 2000. Expression of the nitric oxide synthase 2 gene is not essential for early control of

Mycobacterium tuberculosis in the murine lung. Infect Immun 68: 6879–6882. https://doi.org/10.1128/IAI.68.12.6879-6882.2000.
40. Zhang M, Ming S, Gong S, Liang S, Luo Y, Liang Z, Cao C, Lao J, Shang Y, Li X, Wang M, Zhong G, Xu L, Wu M, Wu Y. 2019. Activation-induced cell death of mucosal-associated invariant T cells is amplified by OX40 in type 2 diabetic patients. J Immunol 203:2614–2620. https://doi.org/10.4049/jimmunol.1900367.
41. Dias J, Boulouis C, Gorin JB, van den Biggelaar R, Lal KG, Gibbs A, Loh L, Gulam MY, Sia WR, Bari S, Hwang WYK, Nixon DF, Nguyen S, Betts MR, Buggert M, Eller MA, Broliden K, Tjernlund A, Sandberg JK, Leeansyah E. 2018. The $CD4^{-}$ $CD8^{-}$ MAIT cell subpopulation is a functionally distinct subset developmentally related to the main $CD8^{+}$ MAIT cell pool. Proc Natl Acad Sci U S A 115:E11513–E11522. https://doi.org/10.1073/pnas.1812273115.
42. Gerart S, Siberil S, Martin E, Lenoir C, Aguilar C, Picard C, Lantz O, Fischer A, Latour S. 2013. Human iNKT and MAIT cells exhibit a PLZF-dependent proapoptotic propensity that is counterbalanced by XIAP. Blood 121: 614–623. https://doi.org/10.1182/blood-2012-09-456095.
43. Jasenosky LD, Scriba TJ, Hanekom WA, Goldfeld AE. 2015. T cells and adaptive immunity to *Mycobacterium tuberculosis* in humans. Immunol Rev 264:74–87. https://doi.org/10.1111/imr.12274.
44. Chua WJ, Truscott SM, Eickhoff CS, Blazevic A, Hoft DF, Hansen TH. 2012. Polyclonal mucosa-associated invariant T cells have unique innate functions in bacterial infection. Infect Immun 80:3256–3267. https://doi.org/10.1128/IAI.00279-12.
45. Darrah PA, Zeppa JJ, Maiello P, Hackney JA, Wadsworth MH, II, Hughes TK, Pokkali S, Swanson PA, II, Grant NL, Rodgers MA, Kamath M, Causgrove CM, Laddy DJ, Bonavia A, Casimiro D, Lin PL, Klein E, White AG, Scanga CA, Shalek AK, Roederer M, Flynn JL, Seder RA. 2020. Prevention of tuberculosis in macaques after intravenous BCG immunization. Nature 577:95–102. https://doi.org/10.1038/s41586-019-1817-8.
46. De Groote MA, Gilliland JC, Wells CL, Brooks EJ, Woolhiser LK, Gruppo V, Peloquin CA, Orme IM, Lenaerts AJ. 2011. Comparative studies evaluating mouse models used for efficacy testing of experimental drugs against *Mycobacterium tuberculosis*. Antimicrob Agents Chemother 55: 1237–1247. https://doi.org/10.1128/AAC.00595-10.
47. Namasivayam S, Maiga M, Yuan W, Thovarai V, Costa DL, Mittereder LR, Wipperman MF, Glickman MS, Dzutsev A, Trinchieri G, Sher A. 2017. Longitudinal profiling reveals a persistent intestinal dysbiosis triggered by conventional anti-tuberculosis therapy. Microbiome 5:71. https://doi.org/10.1186/s40168-017-0286-2.
48. Beste DJ, Espasa M, Bonde B, Kierzek AM, Stewart GR, McFadden J. 2009. The genetic requirements for fast and slow growth in mycobacteria. PLoS One 4:e5349. https://doi.org/10.1371/journal.pone.0005349.
49. Hett EC, Rubin EJ. 2008. Bacterial growth and cell division: a mycobacterial perspective. Microbiol Mol Biol Rev 72:126–156. https://doi.org/10.1128/MMBR.00028-07.
50. Harriff MJ, Cansler ME, Toren KG, Canfield ET, Kwak S, Gold MC, Lewinsohn DM. 2014. Human lung epithelial cells contain *Mycobacterium tuberculosis* in a late endosomal vacuole and are efficiently recognized by $CD8^{+}$ T cells. PLoS One 9:e97515. https://doi.org/10.1371/journal.pone.0097515.
51. Harriff MJ, McMurtrey C, Froyd CA, Jin H, Cansler M, Null M, Worley A, Meermeier EW, Swarbrick G, Nilsen A, Lewinsohn DA, Hildebrand W, Adams EJ, Lewinsohn DM. 2018. MR1 displays the microbial metabolome driving selective MR1-restricted T cell receptor usage. Sci Immunol 3:eaao2556. https://doi.org/10.1126/sciimmunol.aao2556.
52. Huang S. 2016. Targeting innate-like T cells in tuberculosis. Front Immunol 7:594. https://doi.org/10.3389/fimmu.2016.00594.
53. Belmant C, Espinosa E, Poupot R, Peyrat MA, Guiraud M, Poquet Y, Bonneville M, Fournie JJ. 1999. 3-Formyl-1-butyl pyrophosphate A novel mycobacterial metabolite-activating human γδ T cells. J Biol Chem 274:32079–32084. https://doi.org/10.1074/jbc.274.45.32079.
54. Qaqish A, Huang D, Chen CY, Zhang Z, Wang R, Li S, Yang E, Lu Y, Larsen MH, Jacobs WR, Jr, Qian L, Frencher J, Shen L, Chen ZW. 2017. Adoptive transfer of phosphoantigen-specific γδ T cell subset attenuates *Mycobacterium tuberculosis* infection in nonhuman primates. J Immunol 198: 4753–4763. https://doi.org/10.4049/jimmunol.1602019.
55. Chen CY, Yao S, Huang D, Wei H, Sicard H, Zeng G, Jomaa H, Larsen MH, Jacobs WR, Jr, Wang R, Letvin N, Shen Y, Qiu L, Shen L, Chen ZW. 2013. Phosphoantigen/IL2 expansion and differentiation of Vγ2Vδ2 T cells increase resistance to tuberculosis in nonhuman primates. PLoS Pathog 9:e1003501. https://doi.org/10.1371/journal.ppat.1003501.